### MODEL STUDY OF Ca<sup>2+</sup> HANDLING SYSTEMS IN CEREBELLAR GRANULE CELLS

O.E. SAFTENKU
Bohomolets Institute of Physiology, Ukraine
esaft@biph.kiev.ua



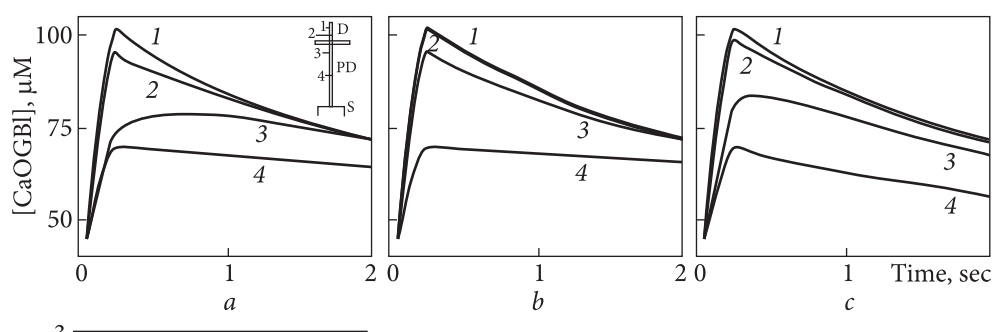
**Dr. O.E. Saftenku** is a graduate of the Department of biophysics at Kyiv State University. She finished a post-graduate course at the Institute of Cybernetics in Kyiv in speciality Control in Biological and Medical Systems, where she received a PhD for her thesis on mechanisms of neuronal bursting activity in central snail neurons. Then she completed a post-doctoral fellowship at the National Heart and Lung Institute in London developing computer models of single calcium channels. Since 1995, she has been working as a researcher at the Department of general physiology of nervous system at the Bohomoletz Institute of Physiology. A variety of her papers are devoted to computational study of single channel kinetics, neurotransmitter dynamics and diffusion in the extracellular environment, short- and long-term plasticity-related synaptic changes, mechanisms of intrinsic excitability, dynamics of intracellular Ca<sup>2+</sup> and Ca<sup>2+</sup> handling systems. Her models are included in international databases.

## Simulation of Ca<sup>2+</sup> gradients in thapsigargin (TG)-treated GrCs

The objective of this study was to investigate the mechanisms that regulate the amplitude, shape, and duration of cytosolic Ca<sup>2+</sup> signals in cerebellar GrCs. A mature GrC has 4 parent dendrites, which end in average with three digits. Gall et al. (2005) showed that the peak amplitudes of fluorescence transients induced by either synaptic stimulation or depolarizing voltage steps progressively and significantly decreased with distance from the dendritic endings. Regional [Ca<sup>2+</sup>]. signals in dendrites are thought to play an important role in the induction of long-term depression and potentiation at the cerebellar MF-GrC synapses, which regulate information transfer at the input layer of the cerebellar cortex. Since spatial heterogeneity of Ca2+ handling systems is thought to be important for defining localized [Ca<sup>2+</sup>], gradients evoked by depolarizing stimuli, the complexity of Ca<sup>2+</sup> regulation makes it difficult to address this problem rigorously. Mathematical modeling represents a useful approach which facilitates testing of various hypotheses and rejection of those ones that fail to match experiment. While this approach alone cannot determine whether a specific distribution of particular Ca<sup>2+</sup> handling systems is necessary to reproduce in the model measured [Ca<sup>2+</sup>],

responses in given cell, it can determine whether such a distribution is sufficient to account for observed  $[Ca^{2+}]_i$  transients. The  $Ca^{2+}$  dynamics was modeled by a set of differential equations. The effects of repetitive stimulation on glutamate release at MF-GrC synapses, glutamate diffusion and NMDA receptor-mediated current in  $Mg^{2+}$ -free solution have been described in our earlier paper (Nieus et al., 2006). We tested various combinations of  $Ca^{2+}$  handling systems (endogenous buffers, calcium channels, extrusion mechanisms, and mitochondria) in the context of a realistic description of GrC morphology and model parameters.

Simulating Ca<sup>2+</sup> responses that were elicited by 200 ms depolarization from -70 to 0 mV in TG-treated GrCs, we have shown that heterogeneities in the distribution of Ca<sup>2+</sup> pumps or in cytosolic fractional volume cannot account for the formation of [Ca<sup>2+</sup>]<sub>i</sub> gradients in GrCs. Observed progressive decay of depolarization-evoked Ca<sup>2+</sup> transients from the dendritic endings to the soma could be reproduced only under suggestion of steep decrease in the calcium current density or large increase in the concentration of endogenous buffers in the dendrites of GrCs from their distal to the proximal parts (Saftenku, 2009a). These two possibilities can be easily distinguished by recordings of fluorescence transients in both parent dendrites and digits with two indicator dyes of different affinities when Ca<sup>2+</sup> uptake and release by internal stores are inhibited (Fig. 1). The total Ca<sup>2+</sup> buffer capacity is the sum of the endogenous and indicator buffer capacities. If the



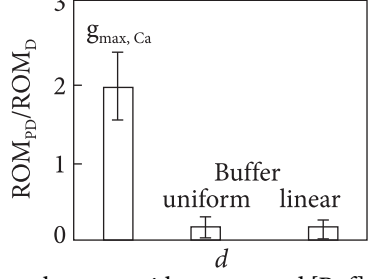


*Fig. 1.* Spatial heterogeneites that can account for Ca<sup>2+</sup> gradients in GrCs; a-c, [CaOGB1] profiles in the digit at locations shown in the inset of (a). In the inset, D is the digit, PD is the parent dendrite and S is the soma. In a — the total buffer concentration [Buf]<sub>T</sub> = 0.95 mM in the digits and soma and [Buf]<sub>T</sub> = 18.7 mM in the parent dendrite. The maximal calcium conductance  $g_{max,Ca} = 2.0 \times 10^{-5}$  S cm<sup>-2</sup> in both cell compartments; b — the buffer concentration increases linearly from the digits

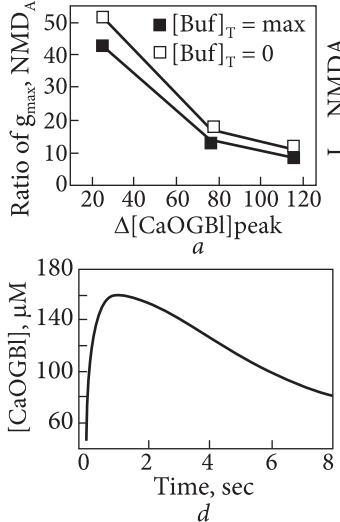
to the soma with an averaged  $[\mathrm{Buf}]_{\mathrm{T}} = 18.7 \,\mathrm{mM}$ . In c — in the digits  $g_{\max,Ca} = 1.93 \times 10^{-5} \,\mathrm{S \, cm^{-2}}$ , in the parent dendrites  $g_{\max,Ca} = 0.52 \times 10^{-5} \,\mathrm{S \, cm^{-2}}$ ,  $[\mathrm{Buf}]_{\mathrm{T}} = 0.8 \,\mathrm{mM}$ ; d — the ROM in the middle of the parent dendrite normalized to the value of ROM in the digit. Vertical bars represent the normalized ROM within the tested ranges of maximum fluorescence change and  $[\mathrm{Buf}]_{\mathrm{T}}$ 

buffer is distributed uniformly, the ratio of the half-decay times of fluorescence transients measured with Oregon Green BAPTA-1 (OGB1) and Mag-Fura-2 (ROM) is always larger in the parent dendrite than in the digit owing to lower  $[Ca^{2+}]_i$  in this cell compartment and the  $Ca^{2+}$ -dependence of the OGB1  $Ca^{2+}$  buffer capacity. But if the buffer with a very large buffer capacity is localized in the parent dendrite, the  $Ca^{2+}$  buffering is dominated by the endogenous  $Ca^{2+}$  buffering capacity. Therefore, the ROM in the parent dendrite is close to one, whereas the ROM is the digits and is expected to be much larger since OGB1 slows significantly the clearance of  $Ca^{2+}$  from the cytosol in the digits of GrCs (Gall et al., 2005).

### Evidences for heterogenous distribution of buffers in GrCs

In the experimental work of Rossi et al. (1994), the peak amplitude of high-voltage-activated calcium currents  $(I_c)$  measured in GrCs acute slices from the cerebellum of rats of the same age (19-23 days) and at the same temperature and other experimental conditions as in the paper of Gall et al. (2005) was 120-150 pA. To compare  $I_{Ca}$  in our model with this current, we multiplied peak  $Ca^{2+}$  current density in each cell compartment by the surface area of this compartment and the number of compartments in a GrC and then summed them. The calculated peak  $I_{Ca}$  in the model with uniformly distributed endogenous buffer appeared to be 13-79 times lower than the experimental  $I_{ca}$ . Such discrepancy could not be explained by the presence of homogeneously distributed endogenous buffers with higher buffer capacity since a half-decay time of fluorescence transients measured in the digits of GrCs with the low-affinity indicator Mag-Fura-2 was 4-8 times shorter compared to the recordings performed with the high-affinity indicator OGB1. Our simulations of NMDA receptor-mediated fluorescence transients in conditions of 1 s stimulation of MFs with frequency 100 Hz, when GrCs were maintained at -70 mV in Mg<sup>2+</sup>-free solution in the presence of the blockers of metabotropic glutamate receptors (mGluRs) revealed that an estimate of the maximum conductance of NMDA receptors per digit which was necessary to reproduce fluorescence changes was also at least 8-50-fold lower than the value estimated from the direct measurement of NMDA receptor-mediated currents in GrCs. When the latter was used in the model, OGB1 was completely saturated.

An increasing Ca<sup>2+</sup> extrusion across the PM in the restricted apical part of the digit could not be suggested since it increased greatly the half-decay time of depolarization-induced fluorescence transients in TG-treated cells. Then we suggested that some immobile buffer could be highly concentrated immediately underneath the sites where MF-GrC synapses and extrasynaptic NMDA receptors are situated. Since calretinin is a predominant calcium buffer in GrCs and it is known to be localized beneath the PM in other cells (Hack et al., 2000), we included in the model a buffer with properties of calretinin. Recent detailed study



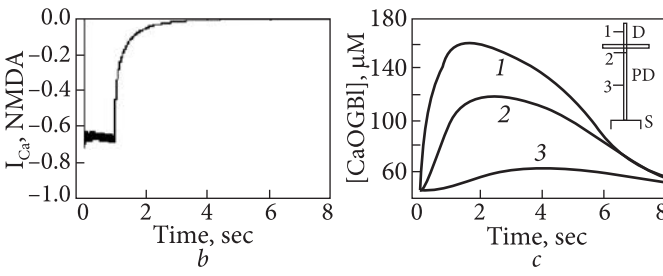


*Fig. 2.* Simulation of synaptically induced fluorescent transients in the presence of mGluR blockers: a — the ratio of an estimate of the maximum conductance of NMDARs per digit ( $g_{max,NMDA}$ ) from direct measurement of NMDAR-mediated currents in GrCs to the  $g_{max,NMDA}$  value which was necessary to reproduce  $\Delta [\text{CaOGB1}]_{\text{peak}}^{1}$  in our model within the range of maximum fluorescence change; b — simulation of the calcium current through NMDAR channels in GrC digit caused by a train of 100 presynaptic stimuli de-

livered at frequency 100 Hz in Mg<sup>2+</sup>-free solution at holding membrane potential -70 mV; c- [CaOGB1] profiles evoked by NMDAR-mediated calcium influx. Calretinin concentration in the apical part of digit was set at 3.1 mM; d- an average [CaOGB1] in the digit when mitochondrial transport with the rate constants of uptake and release 11.4 ms<sup>-1</sup> and  $5.25 \times 10^{-6}$  mM ms<sup>-1</sup>, respectively, were included in the model instead of calretinin

on the binding parameters of calretinin revealed that this buffer has four cooperative binding sites and one independent binding site with different kinetics (Faas et al., 2007). The simulated  $\Delta [CaOGB1]$  reproduced the peak amplitude and the time course of experimental fluorescence transient in the digits in the presence of mGluR blockers when we placed 3-18 mM of calretinin in the most apical compartment of the digit (Fig. 2).

Our simulations show that when an immobilized calretinin is localized only in the apical part of the digits, the ratio of the measured and calculated in the model peak amplitudes of depolarization-induced calcium currents decreases to 4-6 fold. In this case, the maximal Ca<sup>2+</sup> conductance also should be much larger in this compartment than in the rest of the digit. Otherwise a large Ca<sup>2+</sup> flux from the part of the digit where the high-affinity buffer is absent to the part where this buffer is highly concentrated would evoke a very rapid decay of fluorescence transient in the middle of the digit that is not observed.

.Local accumulation of calretinin significantly attenuates global rises of  $[Ca^{2+}]$  in the upper part of the digit and decreases  $Ca^{2+}$  gradients along the digit by a factor of 15 in comparison with uniform distribution of the buffer within the digit. Only such localization of the buffer can be reconciled with a pronounced slowing of the decay of depolarization-induced fluorescence responses in the digits of GrCs after introducing a high-affinity  $Ca^{2+}$  indicator OGB1 (Saftenku, 2009a,b). This situation occurs because the ROM depends not only on the ratio of

total buffer capacities, but also on the  $Ca^{2+}$  axial fluxes determined by the extent of heterogeneity in the distribution of  $Ca^{2+}$  channels along the digit.

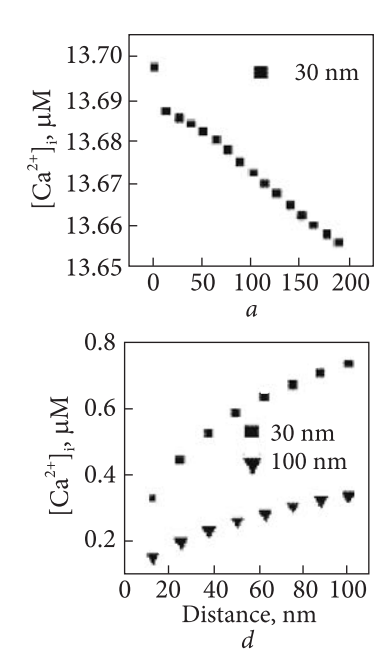
In contrary, the model with 16 mM of calretinin with non-linear binding properties which was concentrated under the plasma membrane of the GrC soma yielded much less attenuation of  $Ca^{2+}$  signals in comparison with the model where the buffer had fast independent binding sites and the same apparent dissociation constant. This occurs because  $Ca^{2+}$  can bind to a cooperative site in the state with a high affinity to  $Ca^{2+}$  only after binding to a site with a low affinity to  $Ca^{2+}$ . Using the model with independent binding sites, we obtained calcium currents with the peak amplitude that was only 1.5-3 times lower than that of typically measured calcium currents. Therefore, it is possible that another high-capacity buffer can be localized in the soma of GrCs. Otherwise the discrepancy between the characteristics of typically measured and simulated depolarization-induced  $I_{Ca}$  are likely to be due to the experimental errors or insufficient statistics.

The functional consequences of calretinin localization in the apical part of the digits, most of all under the plasma membrane, as it was found in the brainstem auditory neurons (Hack et al., 2000), could be an adaptation to large calcium influxes through NMDA-receptor mediated channels. In vivo studies show that the cerebellar MF terminal can fire at over 200 Hz for sustained periods (van Kan et al., 1993) and sustained vesicular release at high rates is preserved at each release site of MF to GrC synapse (Saviane and Silver, 2006). Our estimation of an averaged throughout the cell concentration of immobilized calretinin (57-329 µM) is consistent with the estimate of the concentration of mobile calretinin (1.2-1.3 mM) based on the similarity of its effect on big  $Ca^{2+}$ -activated potassium (BK) channels compared to 150 µM BAPTA (Gall et al., 2003) and the estimates of the calretinin fraction in the cerebellum associated with the particulate fraction (10-27%; Hubbard and McHugh, 1995; Winsky and Kuźnicki, 1995). The association of calretinin with the plasma membrane may promote tight compartmentalization of local Ca<sup>2+</sup> signals and attenuate large [Ca<sup>2+</sup>], responses. In contrast, small [Ca<sup>2+</sup>] responses will not be attenuated at some distance from the sites of Ca<sup>2+</sup> entry because of nonlinear binding properties of calretinin (Faas et al., 2007). These findings explain how GrCs, which are the smallest neurons in the brain and fire in vivo with frequency up to 1000 Hz without accommodating, enable to maintain Ca<sup>2+</sup> homeostasis.

### Influence of calretinin on Ca<sup>2+</sup> microdomains

To explore how calretinin influences  $[Ca^{2+}]_i$  near a single  $Ca^{2+}$  channel, a model of buffered  $Ca^{2+}$  diffusion near a point source that released  $Ca^{2+}$  into a large hemisphere with reflective boundary conditions was considered, Fig. 3.

We used a large concentration of mobile calretinin (1.3 mM) estimated from apparently similar sensitivity of  $Ca^{2+}$ -activated  $K^+$  channels in cerebellar GrCs to



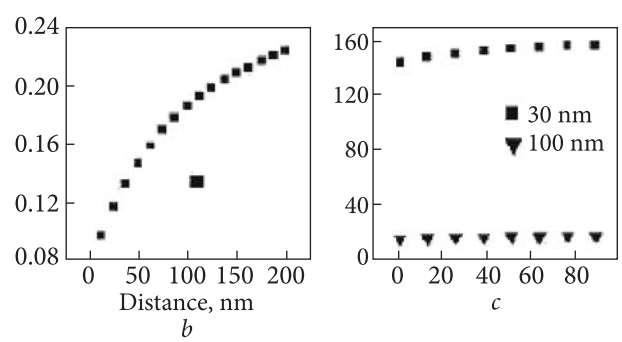


*Fig.* 3. Effect of calretinin on  $Ca^{2+}$  signals evoked by repetitive openings of calcium channels every 12.5 ms (80 Hz).  $[Ca^{2+}]_i$  in the end of each 0.84 ms channel opening (a and c) and immediately before the channel openings (b and d) is shown. The traces were computed with 1.3 mM of mobile calretinin and 3.5 mM of immobile calretinin within 100 nm around a calcium channel. The single channel current amplitude was 0.2 pA (in a and b) and 2 pA (in c and d)

this concentration of the endogenous buffer and to 150  $\mu$ M BAPTA (Gall et al., 2003). The concentration of immobilized calretinin was set to be 3.5 mM within 100  $\mu$ m from an open Ca²+ channel. We showed that the action potential associated increment of free Ca²+ at a distance of 30 nm from the single calcium channel can be reduced by both mobile calretinin and an immobile fraction of this buffer localized underneath the sites of Ca²+ entry through NMDA receptors by 41-54%. Mobile calretinin strongly accelerated the collapse of Ca²+ gradient after channel closure. In contrast to clustered channels, the maximal intracellular free calcium concentration reached during the prolonged repetitive channel openings of the single calcium channel with frequency <80 Hz did not increase because of non-linear properties of calretinin, Fig. 3. It was suggested that in cerebellar GrCs, Ca²+-activated K+ channels can be operated by nanodomains of single N-type Ca²+ channels.

# Ca<sup>2+</sup> release from endoplasmic reticulum and mitochondrial transport

To study the role of mitochondria in shaping  $Ca^{2+}$  transients in GrCs, we used quantitative description of the dependence of mitochondrial transport on the global  $[Ca^{2+}]_i$  developed in the work of Colegrove et al. (2000). Our results show that mitochondrial  $Ca^{2+}$  uptake can decrease the glutamate-induced  $[Ca^{2+}]_i$  elevations in GrCs, but it scarcely influences  $\Delta[Ca^{2+}]_i$  evoked by 200 ms depolarization. However, simulated [CaOGB1] transients evoked by synaptic stimulation had almost twice shorter time to peak ( $\sim$ 1 s) than in the experiment. Inclusion of

inositol-1,4,5-triphosphate (IP $_3$ )-induced Ca $^{2+}$  release in the model resulted in 6-11 % increase in the peak amplitude of the [CaOGB1] transient, which was lower than 25% increase expected from the experiments with the use of mGluR blockers (Gall et al., 2005). In addition, a prominent Ca $^{2+}$  gradient was observed along the digit in these simulations, whereas in the experimental measurements and in the simulations with a high-capacity buffer placed to the apical parts of the digits, the gradient was almost absent.

Mitochondria had a slight additive influence on the amplitude of calcium transients when a high-capacity endogenous buffer was included in the model. The significant delay in time to peak of the [CaOGB1] transient in the digit after termination of synaptic stimulation can be used as an indication onsuch a buffer if it will be observed in the experiments performed in the presence of mGluR blockers and TG. Thus, mitochondrial uptake can explain lower [Ca²+], transients in GrCs than ones expected from typical measurements of NMDAR-mediated current during synaptic stimulation with some additional assumptions such as contribution of CICR to synaptically induced calcium transients and its significant enhancement by IP<sub>3</sub>-induced calcium release. But it cannot explain low depolarization-induced [Ca²+], transients.

Gall et al. (2005) have demonstrated the amplification and protraction of depolarization-induced Ca<sup>2+</sup> entry by Ca<sup>2+</sup>-induced Ca<sup>2+</sup> release (CICR) in the digits of cerebellar GrCs. The results of our simulations are rather consistent with much lower density of the ER in the parent dendrites and soma as compared to the digits of GrCs. When ER transport was added to our model only to the digit compartment, the spatial profiles of experimental fluorescence and simulated [CaOGB1] changes were in close agreement. The long [Ca<sup>2+</sup>], recovery times observed in control cells compared to cells preincubated with TG can be explained by continued CICR with declining rate during the decay phase of Ca<sup>2+</sup> transients. The model based on the interplay between fluxes across the ER and plasma membranes, with decrease of the driving force for passive Ca<sup>2+</sup> release from the ER as the sole mechanism of CICR termination and without inclusion of any inhibitory mechanisms of RyR gating or stochastic attrition can reproduce the main experimental observations. This is consistent with the results of Albrecht et al. (2002) who for the first time separated and described Ca<sup>2+</sup> release and uptake fluxes in intact neurons and showed that the Ca<sup>2+</sup> permeability of the endoplasmic reticulum was not very sensitive to intraluminal Ca<sup>2+</sup> concentration and did not show intrinsic time-dependence.

#### REFERENCES

Albrecht MA, Colegrove SL, Friel DD, 2002. Differential regulation of ER Ca<sup>2+</sup> uptake and release rates accounts for multiple modes of Ca<sup>2+</sup>-induced Ca<sup>2+</sup> release. J. Gen. Physiol 119: 211-233.

Colegrove SL, Albrecht MA, Friel DD, 2000. Quantitative analysis of mitochondrial Ca<sup>2+</sup> uptake and release pathways in sympathetic neurons. Reconstruction of the recovery after depolarization-evoked [Ca<sup>2+</sup>], elevations. J. Gen. Physiol 115: 371-388.

- Faas G.C, Schwaller B, Vergara J.L., Mody I., 2007. Resolving the fast kinetics of cooperative binding: Ca<sup>2+</sup> buffering by calretinin. PLoS Biol 5: e311.
- Gall D, Prestori F, Sola E, D'Errico A, Roussel C, Forti L, Rossi P, D'Angelo E., 2005. Intracellular calcium regulation by burst discharge determines bidirectional long-term synaptic plasticity at the cerebellum input stage. J. Neurosci 25: 4813-4822.
- Gall D, Roussel C, Susa I, D'Angelo E, Rossi P, Bearzatto B, Galas MC, Blum D, Schurmans S, Schiffmann SN, 2003. Altered neuronal excitability in cerebellar granule cells of mice lacking calretinin. J. Neurosci 23: 9320-9327.
- Hack NJ, Write MC, Charters KM, Kater SB, Parks TM, 2000. Developmental changes in the subcellular localization of calretinin. J. Neurosci 20: RC67.
- Hubbard MJ, McHugh NJ, 1995. Calbindin<sub>28kDa</sub> and calbindin<sub>30kDa</sub> (calretinin) are substantially localised in the particulate fraction of rat brain. FEBS Lett 374: 333-337.
- Nieus T, Sola ., Mapelli J, Saftenku E, Rossi P, D'Angelo E, 2006. LTP regulates burst initiation and frequency at mossy fiber–granule cell synapses of rat cerebellum: experimental observations and theoretical predictions. J. Neurophysiol 95: 686-699.
- Rossi P, D'Angelo E, Magistretti J, Toselli M, Taglietti V, 1994. Age-dependent expression of high-voltage activated calcium currents during cerebellar granule cell development in situ. Pflügers Arch 429: 107-116.
- Saftenku EE, 2009a. Computational study of non-homogeneous distribution of Ca<sup>2+</sup> handling systems in cerebellar granule cells. J. Theor. Biol 257: 228-244.
- Saftenku EE, 2009b. Estimation of the capacity of heterogeneously distributed endogenous calcium buffers in a neuron. Neurophysiology 41:131-136.
- Saviane C, Silver RA, 2006. Fast vesicle reloading and a large pool sustain high bandwidth transmission at a central synapse. Nature 439: 983-987.
- van Kan PL, Gibson AR, Houk JC, 1993. Movement-related inputs to intermediate cerebellum of the monkey. J. Neurophysiol 69: 74-94.
- Winsky L, Kuźnicki J, 1995. Distribution of calretinin, calbindin D28k, and parvalbumin in subcellular fractions of rat cerebellum: effects of calcium. J. Neurochem 65: 381-388.